

Control of Linear Vibrations
Automation and Control Laboratory
Politecnico di Milano

Alessio Russo, Gianluca Savaia, Alberto Ficicchia

Academic Year 2015/2016



Contents

The team	iii
Project description	1
I System modelling	2
0.1 Motor, Pinion and Rack modelling	3
0.2 Carts, Springs and Dampers Modelling	3
0.3 1 DOF State Space Model	3
0.4 2 DOF State Space Model	4
0.5 3 DOF State Space Model	5
II System Identification and Filtering	6
0.6 Validation cost function	7
0.7 Open vs Closed loop identification	8
1 White box identification	10
1.1 Detached system: cart and springs identification	10
1.1.1 Experiment description	10
1.1.2 Experiment analysis	11
1.1.3 Experiment results	11
1.1.4 Validation	13
1.2 Motor identification	14
1.2.1 Experiment description	14
1.2.2 Experiment analysis	15
1.2.3 Experiment results	15
1.2.4 Validation	16
1.3 Overall system identification	17
1.3.1 Experiment results	17
1.3.2 Validation	18
2 Gray box identification	21
3 Non-linearities identification	22
3.1 Motor cogging identification	22
3.2 Motor mechanical static friction	22
4 State filtering	24
III System control	25
1 Control of 1 Degree of Freedom	26
1.1 PID and Classical Control	26
1.2 RHP-Zeros Control	26
1.3 H_∞ control	27
1.4 LQG Control	27
1.5 Adaptive control	27
2 Control of 2 Degree of Freedom	28

3 Control of 3 Degree of Freedom	29
Conclusions	30
Appendix	31
Bibliography	31

Team introduction

The team is composed by 3 people, all holding a B.Sci. in Engineering:

1. *Alessio Russo*: holds a B.Sci. degree in Computer Engineering, enrolled at the M.Sci. degree Automation and Control Engineering at Politecnico di Milano. He's also an ASP student, and his thesis will focus on Robust and Adaptive Control of Quadrotors.
2. *Gianluca Savaia*:
3. *Alberto Ficicchia*:

Experience introduction

Part I

System modelling

0.1 Motor, Pinion and Rack modelling

A DC Brushless motor can be modelled with a simple low-pass filter transfer function. Because of that, only a resistance R and an inductance L are needed to model it. Thus, let D be the diameter of the disk attached to the motor, θ the angular position of the disk, J the inertia of the motor, and $c_l(t)$ the load torque. We can also assume non-linearities based on the angle and its rate $\dot{\theta}$: we will denote such non-linearities with $f_m(\theta, \dot{\theta})$.

The output torque of the motor, then, is given by:

$$c(s) = \frac{K_e}{Ls + R}(v(s) - K_e s \theta(s))$$

where $v(s)$ is the Laplace transform of $v(t)$, the input voltage to the motor.

Notice that the term $K_e s \theta(s)$ describes the back-emf effect, though, from experimental results as described 0.7, it's not included in our models. Therefore the output current of the motor, is :

$$i(s) = \frac{1}{Ls + R}v(s)$$

which can be described with a state space model:

$$\begin{cases} \dot{x} = -\frac{R}{L}x + v(t) \\ i = \frac{1}{L}x \end{cases}$$

The differential equation describing the motion of the disk is:

$$J\ddot{\theta} = c(t) - c_l(t) - f_m(\theta, \dot{\theta})$$

In our case, since it's not possible to detach the pinion and the rack from the motor, J includes the inertia of that system, and $c_l(t)$ is the torque load attached to the rack.

The rack position is given by x , which is equal to 0 when the rack is at the center. Since the rack is attached to the disk, and by neglecting non-linear effects such as back-lash, we can say that $x = \frac{D}{2}\theta$. Moreover, the total force transmitted from the motor is:

$$F(t) = c_l(t) = \frac{2}{D}(c(t) - J\ddot{\theta}) = \gamma i(t) - \frac{4}{D^2}J\ddot{x}$$

Where $\gamma = \frac{2K_e}{D}$.

0.2 Carts, Springs and Dampers Modelling

Each cart has the same shape and mass M_c . Let M_i denote the total mass of the i -eth cart including the load, $i \in 1, 2, 3$.

Let x_i be the position of each cart, in cm. The small friction coefficient of the sliding guide can be approximated with a viscous friction $C_s(M)$ which depends on the mass of the cart plus the load.

Finally, each spring is modeled as linear spring. Since we have 3 springs, we have labeled their stiffness as K_l, K_m, K_h where l, m, h stand for low, medium and high. The damping contribute given by each spring is labeled as C_l, C_m, C_h . Therefore let C_i denote the total damping contribution for the i -eth cart.

Therefore, because of Newton's First Law, each cart has equation:

$$M_i\ddot{x}_i + C_i\dot{x}_i + K_i x_i = F(t)$$

Thus, for each cart 2 states are needed to describe its behaviour.

0.3 1 DOF State Space Model

Including the motor 3 states are needed to describe the behaviour of the system. Let x_1 be the state of the motor, x_2 the position of the cart and x_3 its velocity. The measurable state are the first one and the third one, but the

first one needs to be divided by the inductance L as described in the previous section. Therefore the equations to consider are:

$$\begin{cases} \dot{x}_1 = -\frac{R}{L}x_1 + v(t), & i(t) = \frac{1}{L}x_1 \\ \dot{x}_2 = x_3 \\ M\dot{x}_3 = -Cx_3 - Kx_2 + F(t) \end{cases} \quad (1)$$

Since:

$$F(t) = \gamma i(t) - \frac{4}{D^2}J\ddot{x}$$

By letting $\hat{M} = (M + \frac{4}{D^2}J)$, we have:

$$\begin{cases} \dot{x} = \begin{bmatrix} -\frac{R}{L} & 0 & 0 \\ 0 & 0 & 1 \\ \frac{\gamma}{ML} & -\frac{K}{M} & -\frac{C}{M} \end{bmatrix} x + \begin{bmatrix} 1 \\ 0 \\ 0 \end{bmatrix} v(t) \\ y = \begin{bmatrix} \frac{1}{L} & 0 & 0 \\ 0 & 1 & 0 \end{bmatrix} x \end{cases} \quad (2)$$

where $v(t)$ is the external control input.

0.4 2 DOF State Space Model

To derive the equations of motion for the carts we can use the Lagrangian approach.

Let T, V, D be the kinetic, potential and dissipated energy. Then:

$$\begin{aligned} T &= \frac{1}{2} \left(M_1 + \frac{4}{D^2}J \right) \dot{x}_1^2 + \frac{1}{2} M_2 \dot{x}_2^2 \\ V &= \frac{1}{2} k_1 x_1^2 + \frac{1}{2} k_2 (x_2 - x_1)^2 \\ D &= \frac{1}{2} c_1 \dot{x}_1^2 + \frac{1}{2} c_2 (\dot{x}_2 - \dot{x}_1)^2 \end{aligned}$$

Let Q be the external forces acting on the systems:

$$Q = \begin{bmatrix} 1 \\ 0 \end{bmatrix} \gamma i(t)$$

The equations of motion are given by:

$$\frac{d}{dt} \left(\frac{\partial T}{\partial \dot{x}_i} \right) - \frac{\partial T}{\partial x_i} + \frac{\partial V}{\partial x_i} + \frac{\partial D}{\partial \dot{x}_i} = Q_i$$

Thus we can write:

$$\begin{bmatrix} \hat{M}_1 & 0 \\ 0 & M_2 \end{bmatrix} \ddot{x} + \begin{bmatrix} c_1 + c_2 & -c_2 \\ -c_2 & c_2 \end{bmatrix} \dot{x} + \begin{bmatrix} k_1 + k_2 & -k_2 \\ -k_2 & k_2 \end{bmatrix} x = \begin{bmatrix} 1 \\ 0 \end{bmatrix} \gamma i(t)$$

Then:

$$\ddot{x} = M^{-1}C\dot{x} + M^{-1}Kx + M^{-1}B\gamma i(t)$$

where:

$$M = \begin{bmatrix} \hat{M}_1 & 0 \\ 0 & M_2 \end{bmatrix}, C = \begin{bmatrix} c_1 + c_2 & -c_2 \\ -c_2 & c_2 \end{bmatrix}, K = \begin{bmatrix} k_1 + k_2 & -k_2 \\ -k_2 & k_2 \end{bmatrix}, B = \begin{bmatrix} 1 \\ 0 \end{bmatrix}$$

Finally, let x_1 be the state of the motor, x_2 and x_3 the position of the first and second cart, and x_4, x_5 their velocities, then the state space model, is:

$$\begin{cases} \dot{x} = \left[\begin{array}{ccc|cc|cc} -\frac{R}{L} & & & 0 & 0 & 0 & 0 \\ & 0 & & 0 & 0 & 1 & 0 \\ & 0 & & 0 & 0 & 0 & 1 \\ \hline M^{-1}B\frac{\gamma}{L} & & & -M^{-1}K & & -M^{-1}C \end{array} \right] x + \begin{bmatrix} 1 \\ 0 \\ 0 \\ 0 \\ 0 \\ 0 \end{bmatrix} v(t) \\ y(t) = \begin{bmatrix} \frac{1}{L} & 0 & 0 & 0 & 0 \\ 0 & 1 & 0 & 0 & 0 \\ 0 & 0 & 1 & 0 & 0 \end{bmatrix} x \end{cases} \quad (3)$$

where $x \in \mathbb{R}^5$.

0.5 3 DOF State Space Model

As for 2 degree of freedom we can make use again of the Lagrangian Approach:

$$\begin{aligned} T &= \frac{1}{2}(M_1 + \frac{4}{D^2}J)\dot{x}_1^2 + \frac{1}{2}M_2\dot{x}_2^2 + \frac{1}{2}M_3\dot{x}_3^2 \\ V &= \frac{1}{2}k_1x_1^2 + \frac{1}{2}k_2(x_2 - x_1)^2 + \frac{1}{2}k_3(x_3 - x_2)^2 \\ D &= \frac{1}{2}c_1\dot{x}_1^2 + \frac{1}{2}c_2(\dot{x}_2 - \dot{x}_1)^2 + \frac{1}{2}c_3(\dot{x}_3 - \dot{x}_2)^2 \end{aligned}$$

Let Q be the external forces acting on the systems:

$$Q = \begin{bmatrix} 1 \\ 0 \\ 0 \end{bmatrix} \gamma i(t)$$

The equations of motion are given by:

$$\frac{d}{dt} \left(\frac{\partial T}{\partial \dot{x}_i} \right) - \frac{\partial T}{\partial x_i} + \frac{\partial V}{\partial x_i} + \frac{\partial D}{\partial \dot{x}_i} = Q_i$$

Thus we can write:

$$\begin{bmatrix} \hat{M}_1 & 0 & 0 \\ 0 & M_2 & 0 \\ 0 & 0 & M_3 \end{bmatrix} \ddot{x} + \begin{bmatrix} c_1 + c_2 & -c_2 & 0 \\ -c_2 & c_2 + c_3 & -c_3 \\ 0 & -c_3 & c_3 \end{bmatrix} \dot{x} + \begin{bmatrix} k_1 + k_2 & -k_2 & 0 \\ -k_2 & k_2 + k_3 & -k_3 \\ 0 & -k_3 & k_3 \end{bmatrix} x = \begin{bmatrix} 1 \\ 0 \\ 0 \end{bmatrix} \gamma i(t)$$

Then:

$$\ddot{x} = M^{-1}C\dot{x} + M^{-1}Kx + M^{-1}B\gamma i(t)$$

where:

$$M = \begin{bmatrix} \hat{M}_1 & 0 & 0 \\ 0 & M_2 & 0 \\ 0 & 0 & M_3 \end{bmatrix}, C = \begin{bmatrix} c_1 + c_2 & -c_2 & 0 \\ -c_2 & c_2 + c_3 & -c_3 \\ 0 & -c_3 & c_3 \end{bmatrix}, K = \begin{bmatrix} k_1 + k_2 & -k_2 & 0 \\ -k_2 & k_2 + k_3 & -k_3 \\ 0 & -k_3 & k_3 \end{bmatrix}, B = \begin{bmatrix} 1 \\ 0 \\ 0 \end{bmatrix}$$

Finally, let x_1 be the state of the motor, x_2, x_3, x_4 the position of the first, second cart and third cart, and x_5, x_6, x_7 their velocities, then the state space model, is:

$$\left\{ \begin{aligned} \dot{x} &= \left[\begin{array}{c|cc|ccc} -\frac{R}{L} & 0 & 0 & 0 & 0 & 0 & 0 \\ 0 & 0 & 0 & 0 & 1 & 0 & 0 \\ 0 & 0 & 0 & 0 & 0 & 1 & 0 \\ 0 & 0 & 0 & 0 & 0 & 0 & 1 \\ \hline M^{-1}B\frac{\gamma}{L} & -M^{-1}K & -M^{-1}C \end{array} \right] x + \begin{bmatrix} 1 \\ 0 \\ 0 \\ 0 \\ 0 \\ 0 \\ 0 \end{bmatrix} v(t) \\ y(t) &= \begin{bmatrix} \frac{1}{L} & 0 & 0 & 0 & 0 & 0 & 0 \\ 0 & 1 & 0 & 0 & 0 & 0 & 0 \\ 0 & 0 & 1 & 0 & 0 & 0 & 0 \\ 0 & 0 & 0 & 1 & 0 & 0 & 0 \end{bmatrix} x \end{aligned} \right. \quad (4)$$

where $x \in \mathbb{R}^7$.

Part II

System Identification and Filtering

The system considered can be easily modelled and identified without the need to use black-box identification to identify the system.

For completeness both *white-box* and *grey-box* identification are used.

First of all the problem of whether to consider a *closed* or *open* loop system is considered. In fact *back-emf* can be seen as a gain acting on the velocity of the cart, thus it's a gain on the closed loop.

Then, using both *white-box* and *grey-box* identification we identified the main parameters of the system:

1. Resistance and inductance for the motor.
2. Mass, stiffness and damping for the cart and the springs.

Last, identification of non-linearities are considered.

0.6 Validation cost function

An important aspect of the identification process is validation of results and this can be done in many ways.

We will mainly compare two signals, thus effectiveness in capturing the shape of a signal is essential for the type of validation function that we will use.

For this purpose we can make use of a distance function $d(x, y) : \mathbb{R}^n \times \mathbb{R}^n \rightarrow [0, 1]$ induced by a generic norm $n(x) : \mathbb{R}^n \rightarrow [0, \infty)$. In this case we can construct d in the following way:

$$d(x, y) = \frac{1}{1 + n(x - y)}$$

The problem, then, is to find a norm capable of capturing the essential information of a signal.

Usually the L_2 norm is used, since it's related to the signal energy, and from a statistical point of view it corresponds to the variance of the difference of two signals. It's called *MSE-Mean Square Error*: an estimator of the overall deviations between prediction and measurements. Mathematically:

$$\text{MSE} = \mathbb{E}[(x - y)^2]$$

Where n is the dimension of x, y .

Why does it corresponds to the L_2 norm? First of all, notice that $\mathbb{E}[vw]$, where v, w are random variables, corresponds to a non-scaled projection of v on w . Any projection can be written in terms of a generic scalar product $\langle \cdot, \cdot \rangle$, because of the Projection Theorem, thus:

$$\mathbb{E}[(v - w)^2] = \langle v - w, v - w \rangle$$

The last term corresponds to the square of a norm $\|v - w\|^2$, which can be proven to be the L_2 norm:

$$\mathbb{E}[(v - w)^2] = \frac{1}{T} \int_0^T (v - w)^2 dt = \frac{1}{T} \|v - w\|_2^2$$

But does the L_2 norm capture information about the shape of a signal? For signals with finite energy the L_2 norm in time corresponds to a L_2 norm in frequency, due to the Parseval's Theorem. Therefore minimizing the L_2 norm implies the minimization of shape differences between the two signals.

Therefore, *MSE* as defined before, is the square of a norm. Thus:

$$n(z) = \sqrt{\mathbb{E}[z^2]}$$

is a norm. And the validation cost function is:

$$d(x, y) = \frac{1}{1 + n(x - y)} = \frac{1}{1 + \sqrt{\mathbb{E}[(x - y)^2]}}$$

.

0.7 Open vs Closed loop identification

In this experiment we had the necessity to choose whether to consider back-emf in the identification process or to completely ignore it.

As a matter of fact, ignoring it would mean to neglect a feedback component. But how much can it affect identification of other parameters?

Consider for example the following 2-nd order system, such as the system considered in the experiment:

$$G(s) = \frac{1}{Ms^2 + cs + k}$$

First consider a feedback loop with a constant gain ρ on the feedback. Thus the closed loop transfer function is:

$$T(s) = \frac{G(s)}{1 + \rho G(s)} = \frac{1}{Ms^2 + cs + (k + \rho)}$$

The effect of ρ is to change the length of the poles, i.e. their absolute value, since for polynomial with real coefficients the zero-degree coefficient is the product of all roots.

Just compare with $s^2 + 2\xi\omega_0 s + \omega_0^2$, it's easy to see that $\omega_0^2 = \frac{k+\rho}{M}$.

In our case back-emf acts on the velocity of the cart, so if we have a feedback loop on the position, on the feedback we have γs , and the closed loop transfer function is:

$$T(s) = \frac{1}{Ms^2 + cs + k + \gamma s}$$

So what is the effect of γs ? Again, if we compare with $s^2 + 2\xi\omega_0 s + \omega_0^2$ we have:

$$c + \gamma = 2\xi\omega_0$$

Where ξ has a strict relationship with the angle formed between the real negative axis and a pole, θ :

$$\theta = \arctan\left(\frac{\sqrt{1 - \xi^2}}{\xi}\right)$$

So the effect of γs is to rotate the poles, but to which extent is this effect negligible?

From data we are mainly dealing with values of $\xi \in (0, 0.5)$, so we can approximate the value of θ :

$$\theta \approx \arctan\left(\frac{1 - \frac{\xi^2}{2}}{\xi}\right) = \arctan\left(\frac{1}{\xi} - \frac{\xi}{2}\right) \approx \arctan\left(\frac{1}{\xi}\right)$$

Notice that in the last step we made use of the fact that $\frac{1}{\xi} \gg \frac{\xi}{2}$. Check figure 1 to compare the approximation. Then, how much does θ change for a small variation of ξ ?

$$\frac{d\theta}{d\xi} = -\frac{1}{1 + \xi^2} = -1 + \frac{\xi^2}{1 + \xi^2}$$

For $\xi < 0.5$ the change is almost linear, as seen from figure 1. Moreover $\frac{d\theta}{d\xi} \approx -1$ for $0 < \xi < 0.5$, so the slope of the curve is almost -1 .

In our case $\xi = \frac{c+\gamma}{2\omega_0} = \frac{c}{2\omega_0} + \frac{\gamma}{2\omega_0}$, so the contribution of the backemf is $\frac{\gamma}{2\omega_0}$.

From the motor datasheet $\gamma \ll 1$ and from experiments ω_0 is always greater than $10 \frac{rad}{sec}$, therefore the contribution is small, less than 1 and since the contribution to θ is linear with proportion ~ -1 also the change in θ is less than 1 degree, therefore backemf can be ignored and open-loop identification can be applied.

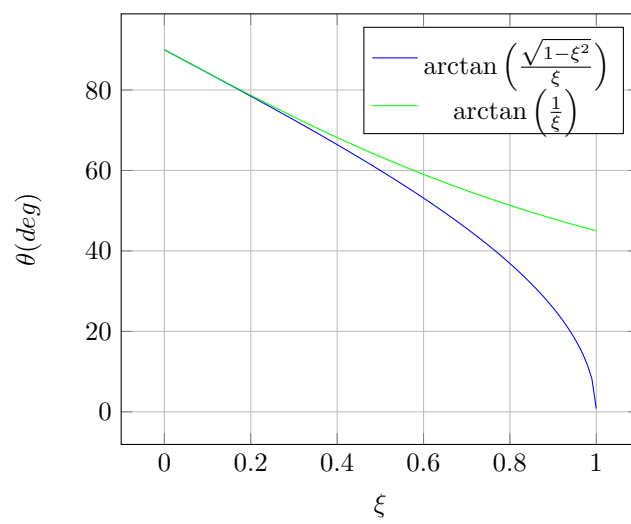


Figure 1: Comparison of the approximated value of θ with the real one

Chapter 1

White box identification

1.1 Detached system: cart and springs identification

To accurately identify the mass of the cart and the stiffness/damping of the spring, the motor was detached from the cart, in order to reduce influence of friction due to the pinion and rack.

So we obtain a system like the one considered in figure 1.1.

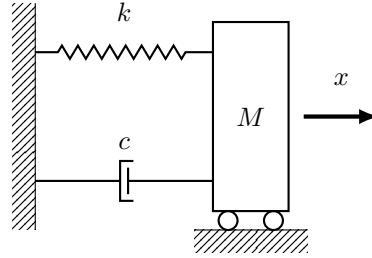


Figure 1.1: Cart detached from the motor diagram.

The differential equation governing this system is given by:

$$M\ddot{x} + c_i\dot{x} + k_ix = f(t)$$

where M [kg] is the total mass of the system, c_i [Ns m^{-1}] comprehends the damping of the i -eth spring and the viscous damping of the sliding guide. Finally k_i [N m^{-1}] is the stiffness of the i -eth spring, and $f(t)$ represents external forces acting on the system (such as non-linear friction components).

1.1.1 Experiment description

For each spring we conducted 2 experiments, one without any load and one with a load of 0.986 [kg], each repeated 3 times. To accurately identify the mass of the cart and the stiffness/damping of the spring, the motor was detached from the cart, in order to reduce influence of friction due to the pinion and rack.

For each experiment the cart was released from an initial condition $x(0) = x_0 \neq 0$ and 0 velocity, such that the force that the spring was exerting on the cart was sufficient enough to make negligible the very small component of the static friction acting on the cart.

Notice that the initial condition differs for each spring since the stiffness is very different for each spring.

If we neglect the external forces acting on the cart, which are negligible since they are small non-linear components, then the system considered is:

$$\begin{cases} M\ddot{x} + c_i\dot{x} + k_ix = 0 \\ x(0) \in [1, 3]\text{cm} \\ \dot{x}(0) = 0 \end{cases} \quad (1.1)$$

Then data regarding the position of the cart is collected, and from that data the pulsation, damping ratio, mass and stiffness are retrieved.

1.1.2 Experiment analysis

Using 1.1 the response in time can be obtained by using the Laplace transform. Let $X(s)$ be the Laplace transform of $x(t)$, then:

$$mX(s)(s^2 - x(0)s) + cX(s)(s - x(0)) + kX(s) = 0$$

and:

$$X(s) = x(0) \frac{(ms + c)}{ms^2 + cs + k}$$

If we solve in $X(s)$ and then apply the inverse Laplace transform, we obtain the response in time:

$$x(t) = e^{-\xi\omega_0 t} (A \cos(\omega t) + B \sin(\omega t))$$

where $\xi = \frac{c}{2\sqrt{Mk}}$, $\omega_0 = \sqrt{\frac{k}{M}}$, $\omega = \omega_0 \sqrt{1 - \xi^2}$, and A, B depend on $x(0), \xi$.

Since the pulsation is the same for both sinusoidal components we have:

$$x(t) = Ce^{-\xi\omega_0 t} \sin(\omega t + \phi)$$

Where $C = \sqrt{A^2 + B^2}$, $\phi = \arctan(A/B)$.

Knowing those equations we are able to extract data from the response in the following way:

- To measure ω we can just extract the period T : the difference in time between the first and second peak is taken, and that difference is the period. Then ω is just $\frac{2\pi}{T}$. We consider only the first and second peak because at the beginning non-linearities such as static and coulomb friction are negligible.
- To measure ξ also the first and second peak are considered. Let t_0, t_1 be the times at which there is the first and second peak. Notice that $t_0 = 0, t_1 = T$, and $x(T) = Ae^{-\xi\omega_0 T}$. Then, consider:

$$\log\left(\frac{x(0)}{x(T)}\right) = \log(e^{\xi\omega_0 T}) = \xi\omega_0 T = \frac{\xi}{\sqrt{1 - \xi^2}} 2\pi$$

Then

$$\xi = \frac{a}{\sqrt{a^2 + 1}}, \quad a = \frac{1}{2\pi} \log\left(\frac{x(0)}{x(T)}\right)$$

Once M, k are known we can calculate the damping from $c = 2\xi\sqrt{Mk}$. Observe that for $a \sim 0 \Rightarrow \xi \sim a$. Since damping

- To identify each spring and the mass of the cart we made use of the fact that we have two type of experiments for each spring: one without any load, and one with a load of 0.986 kg. We obtain a system of linear equations:

$$\begin{cases} \frac{k_i}{m_c + m_l} = \omega_l^2 \\ \frac{k_i}{m_c} = \omega_{nl}^2 \end{cases}$$

Where m_c is the mass of the cart, m_l the mass of the load, ω_l the pulsation of the system with the load, ω_{nl} the pulsation of the system without the load. It's a system with two unknowns (k_i, m_c) and two equations, so we can solve it. We can rewrite it in matrix form:

$$\begin{bmatrix} 1 & -\omega_l^2 \\ 1 & -\omega_{nl}^2 \end{bmatrix} \begin{bmatrix} k_i \\ m_c \end{bmatrix} = \begin{bmatrix} \omega_l^2 m_l \\ 0 \end{bmatrix}$$

and solve for (k_i, m_c) .

1.1.3 Experiment results

Since there are 3 springs let's denote the set of springs as $K = \{k_l, k_m, k_h\}$ where l stands for low, m for medium and h for high. In a similar manner we define the various pulsation: for example ω_{m-nl} is the pulsation for the system with spring k_m and no load.

Pulsation In the table below are shown the various mean of the pulsation and their relative standard deviation:

It's interesting to note that even if we considered to average all the periods by considering the various peaks of the signal, and not only the first two peaks, we would have obtained the same results. This is an hint of the fact that the principal non-linearity, i.e. coulomb friction, is negligible.

$(\omega_{avg} [\text{rad s}^{-1}], \omega_{std} [\text{rad s}^{-1}])$	k_h	k_m	k_l
with load	(21.2989, 0)	(14.2800, 0.0671)	(10.6495, 0)
with no load	(34.9066, 0)	(23.7101, 0.1792)	(17.6991, 0.1005)

Table 1.1: Pulsation of the cart detached from the motor. Various configuration are shown (with a load of 0.986 [kg] and no load) for the various springs.

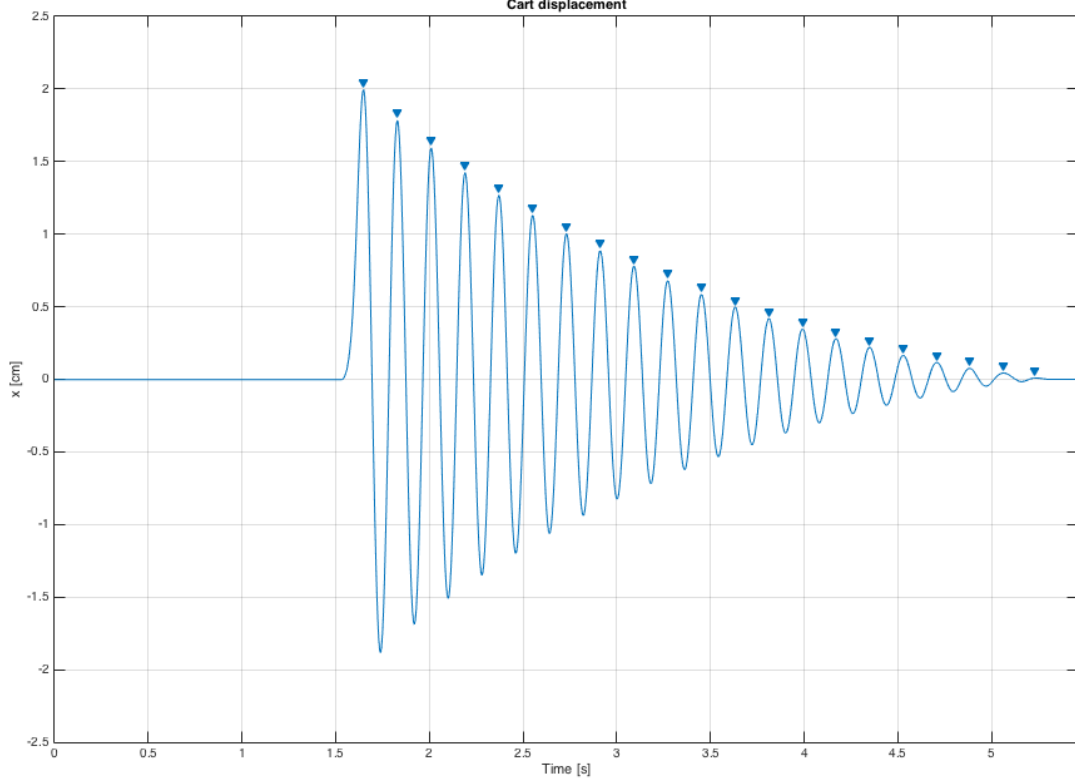


Figure 1.2: Displacement of the cart with spring k_h and load 0.986 [kg].

Cart mass and springs stiffness By using mean pulsation the resultant average mass of the cart m_c is 0.5685 [kg] with standard deviation 0.0141 [kg]. Results also for the springs are shown in table ??.

$(k_h [\text{N m}^{-1}], m_c [\text{kg}])$	$(k_m [\text{N m}^{-1}], m_c [\text{kg}])$	$(k_l [\text{N m}^{-1}], m_c [\text{kg}])$
(712.5990, 0.5848)	(315.5074, 0.5612)	(175.2819, 0.5595)

Table 1.2: Identified springs and cart mass

Damping and damping ratio The mean values for the damping ratio, including their standard deviation, are shown in table ?? for the various springs, with and without a load.

(ξ_{avg}, ξ_{std})	k_h	k_m	k_l
with load	(0.0128, 0.0007)	(0.0238, 0.0018)	(0.0346, 0.0036)
with no load	(0.0179, 0.0025)	(0.0301, 0.0013)	(0.0379, 0.0040)

Table 1.3: Damping ratio. Various configuration are shown (with a load of 0.986 [kg] and no load) for the various springs.

From the values shown in table ?? it seems that the damping C is function of the mass, in fact we don't obtain the same damping if we consider the damping ratio with no load or with load. For example consider k_h : with a load we obtain $C = 0.0128 \cdot 2 \cdot \sqrt{k_h M} = 0.8520 [\text{N s m}^{-1}]$, without load: $C = 0.0179 \cdot 2 \cdot \sqrt{k_h m_c} = 0.7206 [\text{N s m}^{-1}]$. This is most likely an effect due to friction, and the various damping values are shown in table ??.

C [N s m ⁻¹]	k_h	k_m	k_l
with load	0.8520	1.0542	1.1423
with no load	0.7206	0.8063	0.7567

Table 1.4: Damping values. Various configuration are shown (with a load of 0.986 [kg] and no load) for the various springs.

We can therefore linearly characterize the damping value as function of the mass centered in m_c , for each spring:

$$C(m) = C_{nl} + \frac{C_l - C_{nl}}{m_l}(m - m_c) = C_{nl} + \alpha(m - m_c)$$

The different values of α , the difference quotient, are shown in table ??

$\frac{C_l - C_{nl}}{m_l}$ [N s m ⁻¹ kg ⁻¹]	k_h	k_m	k_l
	0.1334	0.2514	0.3911

Table 1.5: Damping difference quotient. Due to friction damping changes for different weights, we can therefore characterize the damping in a linear way with the formula: $C(m) = C_{nl} + \frac{C_l - C_{nl}}{m_l}(m - m_c) = C_{nl} + \alpha(m - m_c)$. Values of the difference quotient are shown for the different springs.

1.1.4 Validation

Validation was done in a similar fashion as the experiments conducted to identify the system parameters. The cart was released from a random initial condition x_0 and then released.

Measurements were compared with the output simulation of a model constructed from the identified parameters, and results were compared with the cost function defined in 0.6.

On average, the cost function, on a scale from 0 to 1, gave a fit of 0.9449 with standard deviation 0.0263. The minimum was 0.8778, and maximum 0.9716.

In figure 1.7 it is visible that due to unmodelled effects, such as friction and stiffness not being exactly linear, there is a loss of accuracy on the long run, but accuracy is very high in the beginning, where non-linearities are not relevant yet. Thus it is safe to assume that the parameters of the cart are the ones identified by this experiment.

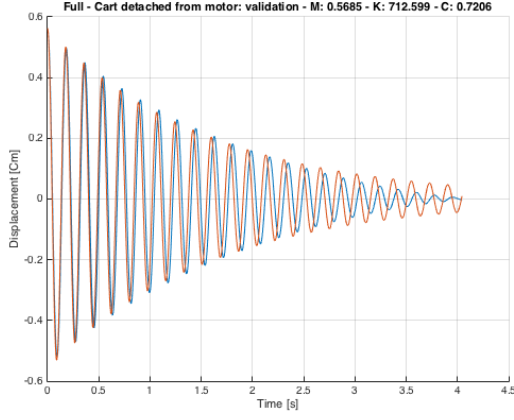


Figure 1.3: Validation test without load and K_h .

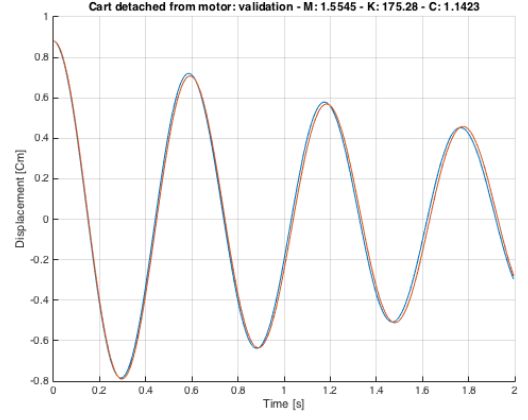


Figure 1.4: Validation test without load and K_l .

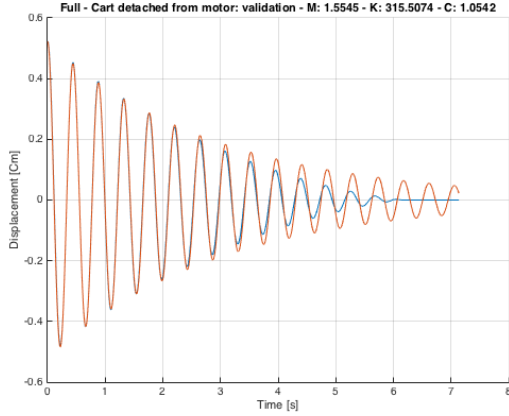


Figure 1.5: Validation test with load and K_m .

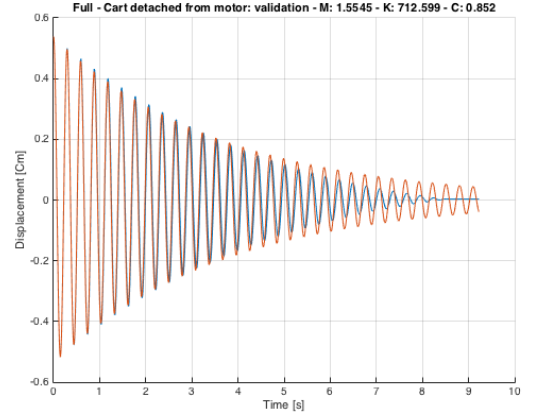


Figure 1.6: Validation test with load and K_h .

Figure 1.7: Validation tests of the cart detached from the motor. In orange the simulated output, in blue the measurement of the validation test. Effect of friction is clearly visible, such as in 1.5, where the cart stops after 6 seconds.

1.2 Motor identification

The motor can be modelled as a first order low pass filter, and the main parameters are:

- Resistance of the motor, R [Ω].
- Inductance of the motor, L [H].
- Torque constant, K_e [N m A^{-1}].

From motor specifications the nominal values, which are identified with n as subscript, are:

$$R_n = 1.4[\Omega], L_n = 0.0021[H], K_{en} = 0.118[\text{N m A}^{-1}]$$

The nominal cut-off frequency of the motor is $f_n = \frac{R_n}{L_n} = 106.10$ [Hz], which is slightly above the Nyquist frequency of the system 100 [Hz], therefore accurate identification by means of grey or black box identification may give a bias on the identification of the cut-off frequency.

Since resistance of the motor can be identified by steady state value of the current, only inductance may have a biased value.

1.2.1 Experiment description

For each spring K_i , two experiments were done, with the motor attached to the cart, one with a load of 0.986 kg, and one without any load (just the cart itself).

Since we can measure the current and because of our assumption that back-emf can be ignored (hence the system is open-loop), we can directly identify the motor from the input voltage and the output current. Moreover, back-emf doesn't influence the steady state value of the current (since it acts on the velocity of the cart, which is 0 at steady state), therefore resistance of the motor can be accurately identified. Regarding the inductance, we can not accurately identify it, since because of our sampling time the motor can almost be considered like a gain system. Therefore rising time and the use of estimation techniques will be used.

The input voltage is a square wave with period 10:

$$v(t) = \begin{cases} a, & t \in [t_0, t_0 + 5] \\ -a, & t \in [t_0 + 5, t_0 + 10] \end{cases}$$

where t_0 is the beginning time of the square wave, and $a = 3$ for K_h, K_m and $a = 2$ for K_l . In fact the current is proportional to the output torque of the motor, which ultimately acts on the cart which is attached with a spring to a wall, therefore less voltage is needed for springs with low stiffness to move the cart.

The system to be considered is:

$$L\dot{i}(t) + Ri(t) = v(t)$$

Where $i(t)$ is the current measured from the motor.

Finally, each experiment was run for a period of time of about ≈ 40 [s].

1.2.2 Experiment analysis

The system considered is a stable system, therefore at steady state $\dot{i}(t) = 0$ and $R = \frac{v(t)}{i(t)}$.

Because of noise sensor the mean value was taken as steady state value, after the transient due to back-emf. Since we know the input voltage we can then calculate R .

Regarding the inductance, since the motor can be modelled as a low pass filter of the first order, its response in time has the form $i(t) = v(1 - e^{-\tau t})$, where $\tau = \frac{R}{L}$. When $t = \frac{3}{\tau}$, which is about our sampling time since $\frac{3}{\tau_n} = \frac{3}{2\pi f_n} \approx 0.0045$ [rad s⁻¹], we have $i(\frac{3}{\tau}) \approx 0.95v$. Therefore we can check if after one time step the value is approximately 0.95 times the value of the input voltage.

Ultimately we can use the function *tfest* in matlab to identify a system of the first order given the input and output data.

1.2.3 Experiment results

From experiments steady state value of the current seems to change a little, based on the fact whether v is positive or negative. Thus let R_1 represent mean value of resistance when v is positive, and R_2 when v is negative.

From data mean values are: $R_1 = 1.3069$ [Ω], $R_2 = 1.2330$ [Ω], with standard deviation $\sigma_1 = 0.0984\Omega$, $\sigma_2 = 0.0460\Omega$.

R then can be computed using a weighted average:

$$R = \frac{\sigma_2^2 R_1 + \sigma_1^2 R_2}{\sigma_1^2 + \sigma_2^2} = 1.2462\Omega$$

And standard deviation:

$$R_{std} = \sqrt{\frac{\sigma_1^2 + \sigma_2^2}{2}} = 0.0059\Omega$$

Using the *tfest* command the average and standard deviation values for R, L are:

$$R = 1.2689\Omega, R_{std} = 0.0562\Omega$$

$$L = 0.0024\text{H}, L_{std} = 0.0002\text{H}$$

Using again a weighted average the mean value of R is $R = 1.2464\Omega$ with standard deviation 0.04Ω .

Regarding the inductance, the estimated value fits the nominal value. This can also be seen from figure 1.9 that steady state is approached in about 2 steps of the sampling time.

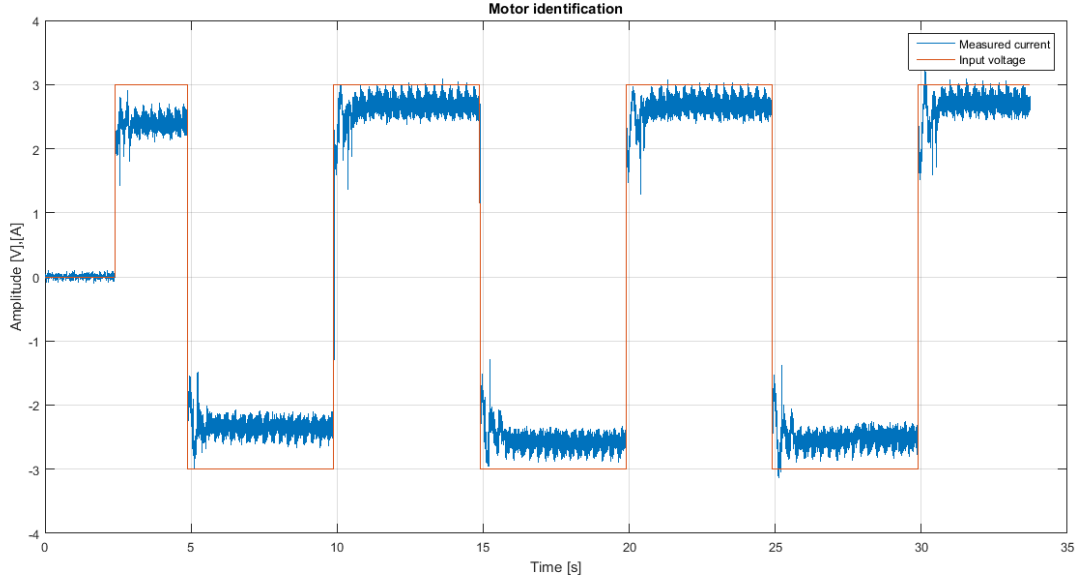


Figure 1.8: Input voltage and output current of the motor

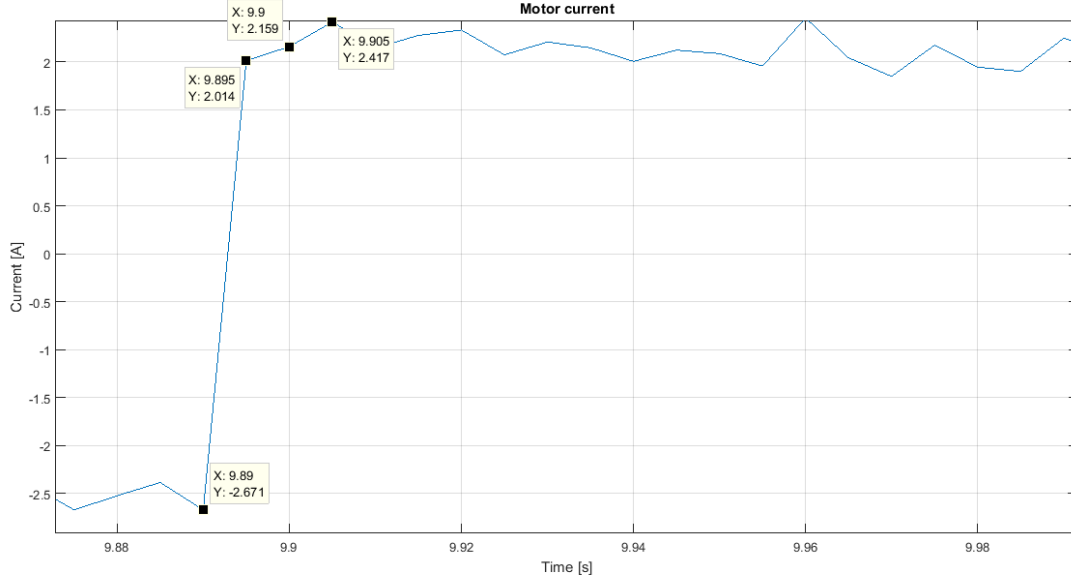


Figure 1.9: Rising time of the current, it can be seen that steady state is approached very quickly.

1.2.4 Validation

Validation was done using a random input with normal distribution $N(0, \frac{9}{4})$ (Check figure 1.10). Notice that we couldn't have used that input as source for identification because we already know a model of the system, and so we are not interested in black box modeling.

On average, using the cost function defined in 0.6, with a first order system of the type:

$$G(s) = \frac{1}{Ls + R}$$

where $R = 1.2689\Omega$, $L = 0.0024H$, there is an average fit value $d(i_{real}, i_{sim}) = 0.8142$ with standard deviation 0.0364. In case black box identification is used, with a 3rd order system we would obtain an average fit value of 0.8527 with standard deviation 0.0424.

In case we consider a pulse input then the fit value obviously increase over 0.9, thus the results obtained are acceptable.

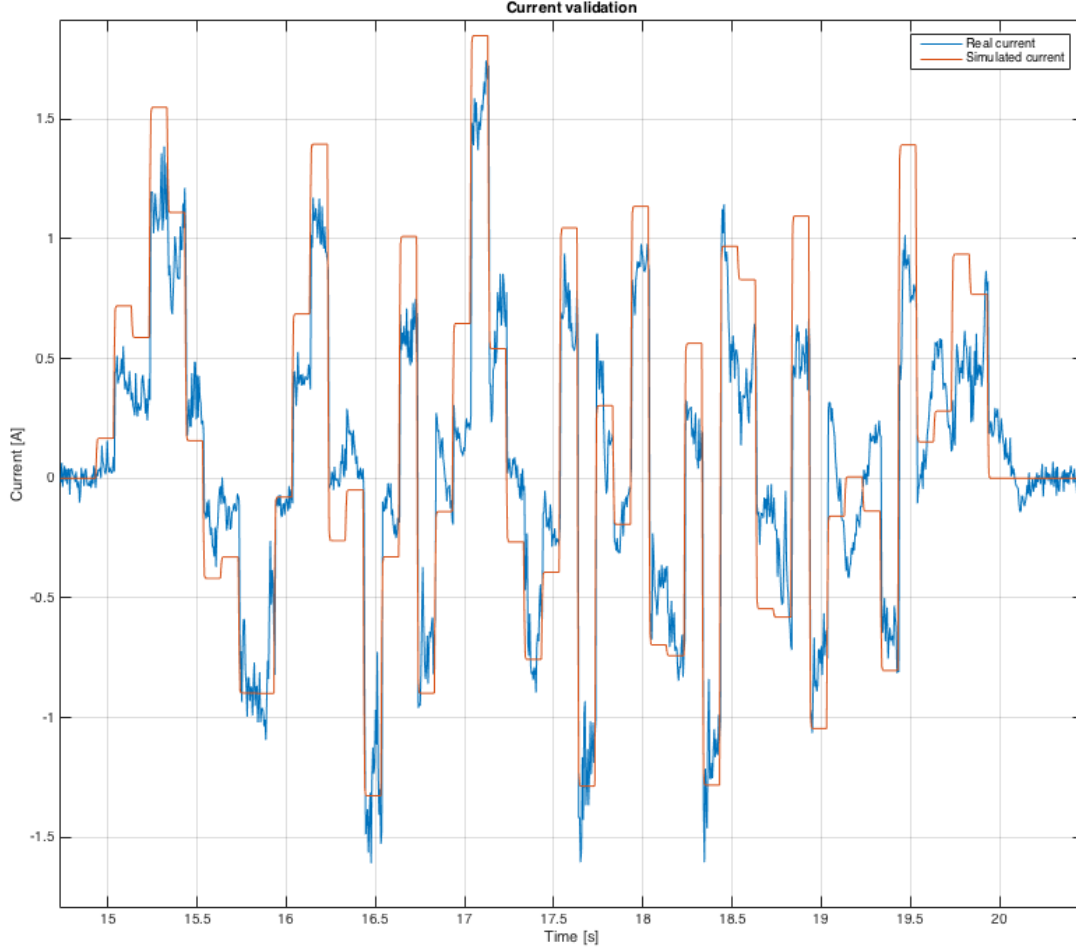


Figure 1.10: Validation of the motor with a random input signal $v(t) \sim N(0, \frac{9}{4})$.

1.3 Overall system identification

The system was modelled as an open loop system as specified in section 0.6. We have mainly a series connection of two systems: the motor and the cart, which are identified by the following transfer functions:

$$G_1(s) = \frac{1}{Ls + R} \quad G_2(s) = \frac{\gamma}{Ms^2 + Cs + K}$$

Since we are using the same tests used to identify the motor (section 1.2), and the same techniques used to identify the cart detached from the motor (section 1.1), those two sections are not presented.

1.3.1 Experiment results

Results are summarized in a similar fashion to section 1.1:

Pulsation In the table below are shown the various mean of the pulsation of the cart and their relative standard deviation:

$(\omega_{avg} [\text{rad s}^{-1}], \omega_{std} [\text{rad s}^{-1}])$	k_h	k_m	k_l
with load	(20.2100, 0.0022)	(13.0633, 0.3208)	(10.7500, 0.0308)
with no load	(30.4300, 0.2895)	(18.3767, 0.2011)	(15.6240, 0.1820)

Table 1.6: Pulsation of the cart attached to the motor. Various configuration are shown (with a load of 0.986 [kg] and no load) for the various springs.

System gain, mass and stiffness By using mean pulsation the resultant average mass of the system, including the cart, is 0.8906 [kg] with standard deviation 0.1146 [kg]. Results also for the stiffness are shown in table ?? . Therefore it results that the mass contribution of the motor is:

$(k_h \text{ [N m}^{-1}\text{]}, m \text{ [kg]})$	$(k_m \text{ [N m}^{-1}\text{]}, m \text{ [kg]})$	$(k_l \text{ [N m}^{-1}\text{]}, m \text{ [kg]})$
(720.56, 0.778)	(340.14, 1.007)	(216.38, 0.8864)

Table 1.7: Identified stiffness and mass of the overall system

$$M_{motor} = 0.8906 - 0.5685 = 0.3221\text{Kg}$$

The identified gain of the motor, based on the fact that at steady state we have:

$$x(\infty) = \frac{\gamma}{k}i(\infty)$$

gives an average value of $\gamma = -2.0680 \text{ N A}^{-1}$ and standard deviation $\gamma_{std} = 0.2935 \text{ N A}^{-1}$. Notice that $x(\infty), i(\infty)$ refers to the corresponding value at steady state.

Damping and damping ratio The mean values for the damping ratio, including their standard deviation, are shown in table ?? for the various springs, with and without a load.

(ξ_{avg}, ξ_{std})	k_h	k_m	k_l
with load	(0.1356, 0.00022)	(0.1949, 0.0080)	(0.2230, 0.0042)
with no load	(0.1670, 0.0084)	(0.2569, 0.0124)	(0.2973, 0.0376)

Table 1.8: Damping ratio. Various configuration are shown (with a load of 0.986 [kg] and no load) for the various springs.

From the values shown in table ?? it seems that the damping C is function of the mass, like in ??. The various damping values are shown in table ??.

$C \text{ [N s m}^{-1}\text{]}$	k_h	k_m	k_l
with load	10.2855	9.5558	8.9973
with no load	9.0517	8.4089	8.2736

Table 1.9: Damping values. Various configuration are shown (with a load of 0.986 [kg] and no load) for the various springs.

We can therefore linearly characterize the damping value as function of the mass centered in m_c , for each spring:

$$C(m) = C_{nl} + \frac{C_l - C_{nl}}{m_l}(m - m_c) = C_{nl} + \alpha(m - m_c)$$

The different values of α , the difference quotient, are shown in table ??

	k_h	k_m	k_l
$\frac{C_l - C_{nl}}{m_l} \text{ [N s m}^{-1} \text{ kg}^{-1}\text{]}$	1.2514	1.1631	0.7340

Table 1.10: Damping difference quotient. Due to friction damping changes for different weights, we can therefore characterize the damping in a linear way with the formula: $C(m) = C_{nl} + \frac{C_l - C_{nl}}{m_l}(m - m_c) = C_{nl} + \alpha(m - m_c)$. Values of the difference quotient are shown for the different springs.

1.3.2 Validation

For the validation procedure we used the same input voltage used in the validation of the motor, section 1.2.4. $v(t) \sim \alpha N(0, \frac{9}{4})$, where $\alpha \in (0.7, 1.5)$ based on which spring was attached to the first cart.

Validation 1 DOF

For each spring we made two tests, one without load and one with a load of about 1kg, for a total of 6 tests. Validation using only one cart can be summarised in an average fit value of 85.42 %, with standard deviation of 1.68 %. Because of such high value, there is no need to consider more details in the models such as back-emf or nonlinearities.

In figure 1.15 some validation plots are shown.

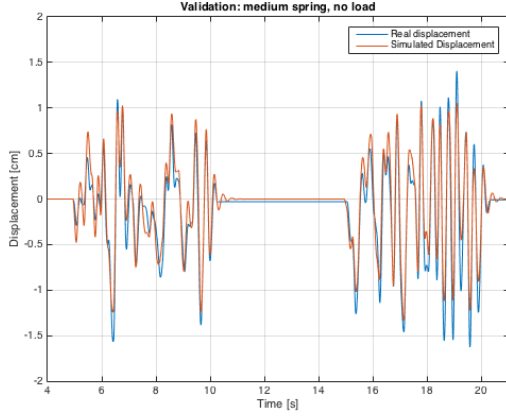


Figure 1.11: Validation test without load and K_m .

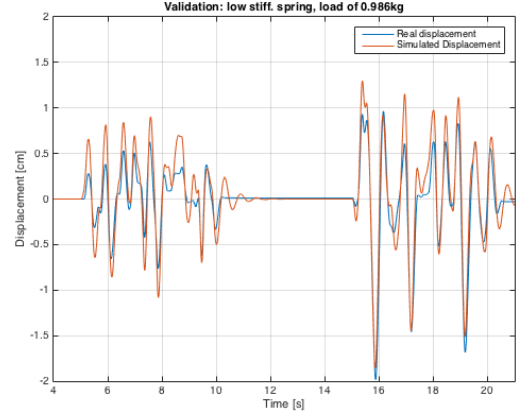


Figure 1.12: Validation test with load and K_l .

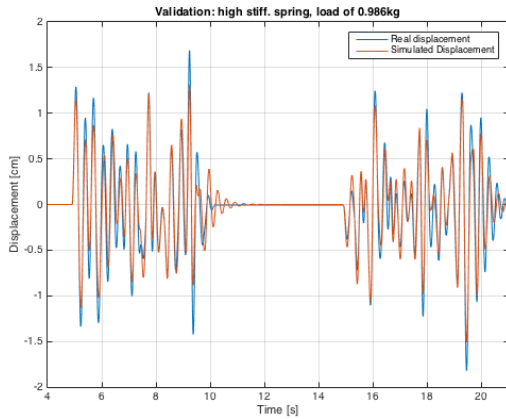


Figure 1.13: Validation test with load and K_h .

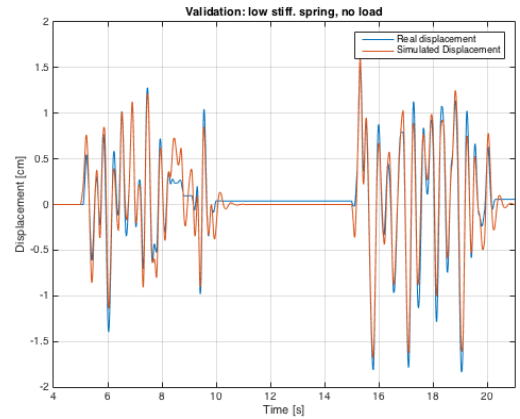


Figure 1.14: Validation test with no load and K_l .

Figure 1.15: Validation tests of the cart attached to the motor. In orange the simulated output, in blue the measurement of the validation test.

Validation 2 DOF

Validation for 2 degree of freedom used the same random distribution of the validation input for 1 degree of freedom. We tested the combination K_h, K_m and K_l, K_h . For each combination we made 3 tests, one without any load on the two carts, one with half kilogram on each cart, and one with 1 kilogram only on the second cart. Since now we have 2 outputs, the position of the first and second cart, we need to average the results for the first and second cart.

For the first cart we have an average fit of 87.29 % with standard deviation 4.5%. For the second cart the average fit is 85.79%, with standard deviation 4.8 %.

This results in a mean of 86.54 %, and standard deviation 4.68 %. Some validation plots are shown in figure 1.20 for the second cart.

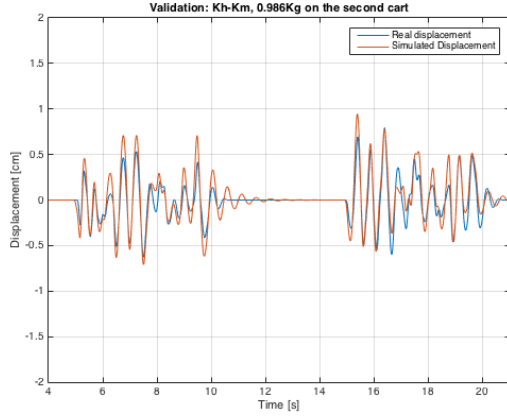


Figure 1.16: Validation test without load on the first cart, and a load of 0.986kg on the second one. The configuration K_h, K_m was used.

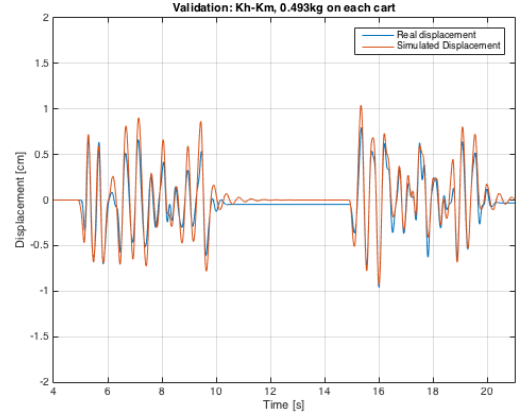


Figure 1.17: Validation test a load of about 0.493 kg on both the carts. The configuration K_h, K_m was used.

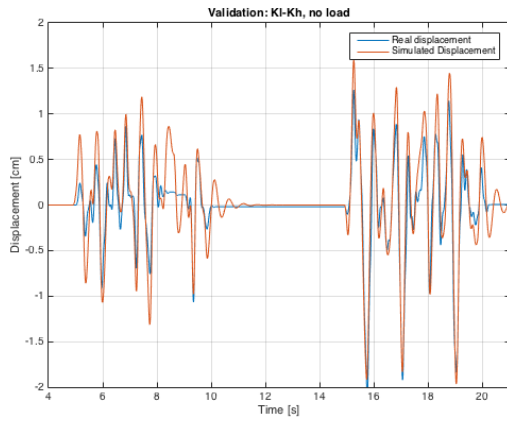


Figure 1.18: Validation test with no load on both the carts. The configuration K_l, K_h was used.

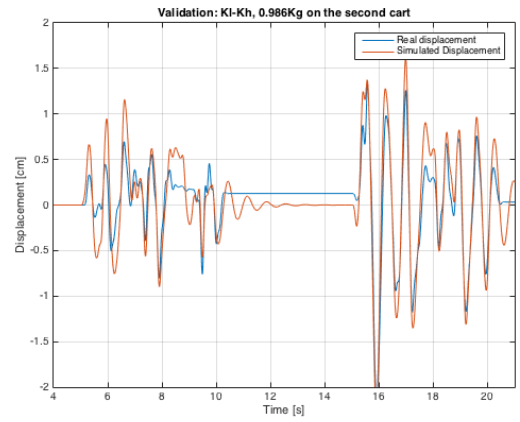


Figure 1.19: Validation test without load on the first cart, and a load of 0.986kg on the second one. The configuration K_l, K_h was used.

Figure 1.20: Validation tests of 2 degree of freedom. Only the output for the second cart is shown. In orange the simulated output, in blue the measurement of the validation test.

Chapter 2

Gray box identification

Chapter 3

Non-linearities identification

3.1 Motor cogging identification

It was found that for low voltage the motor acts as if the voltage is 0, therefore the current and consequently the torque is 0.

This is a type of static friction, though it's not a mechanical one. In fact, if it was a mechanical one we would see the current increase but the shaft of the motor don't rotate until the torque is big enough to counteract the static friction effect. In this case is more an electrical type of static friction, called *cogging* effect.

COPIATO DA WIKI

Cogging torque of electrical motors is the torque due to the interaction between the permanent magnets of the rotor and the stator slots of a Permanent Magnet (PM) machine. This torque is position dependent and its periodicity per revolution depends on the number of magnetic poles and the number of teeth on the stator. Cogging torque results in torque as well as speed ripple; however, at high speed the motor moment of inertia filters out the effect of cogging torque.

In figure 3.1 such effect is shown. On the left plot it's visible that when the input voltage $v(t)$ for $|v(t)| < c$, the output current is 0. Since the torque is proportional to the current, also the torque is 0. On the right plot is visible the effect on the cart: when the cart starts to move, after having overcome the static friction, it stops because the torque goes to 0 because the current is 0. But this effect does not happen because of mechanical static friction, otherwise we would not see a flat current curve.

How can we model such effect? It's some kind of dead-zone effect, and we can model it such that the real voltage entering the motor is:

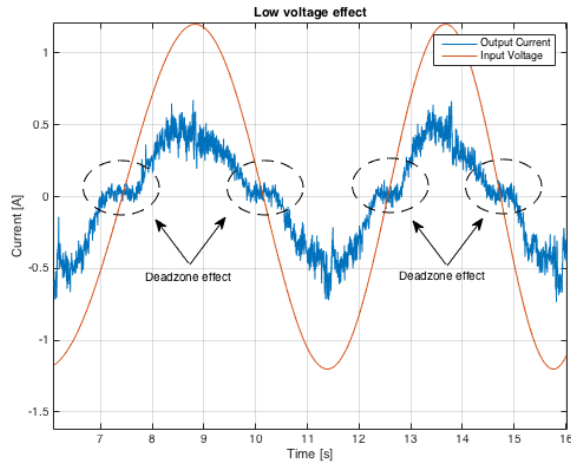
$$v_{real}(t) = \begin{cases} 0 & |v(t)| < c \\ v(t) & |v(t)| \geq c \end{cases} \quad (3.1)$$

Where $c \in \mathbb{R}$ needs to be identified. For this purpose, notice that inside the dead-zone the current is a white noise signal. Therefore we should find a constant α such that the signal $|i(t)| < \alpha$ is a white noise signal. We can make use of the fact that $v(t) \in C^\infty$ signal, find a set $\hat{t} = \{t \in \mathbb{R} : |v(t)| < c\}$ and check the whiteness of the current in that set \hat{t} . Since v is continuous, that set is measurable (using the Lebesgue measure). Also the current is continuous, therefore it's also continuous on that set. For this purpose the following identification procedure was used:

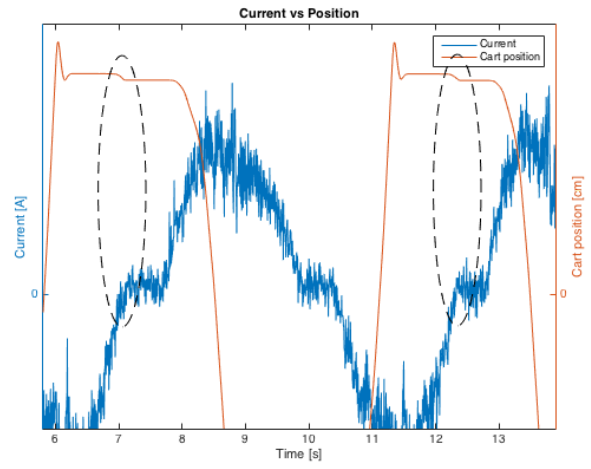
1. Use as voltage input a sinusoid with frequency pulsation $\omega = 1.25 \text{ rad s}^{-1}$.
2. Choose $c \in [0, \max(v(t))]$, where $v(t)$ is the input voltage. Consider only the voltage that satisfies $|v(t)| < c$.
3. Run the Anderson Whiteness Test on the current for those values of t where $|v(t)| < c$, with margin of tolerance of 1%.
4. If the signal is not white, run again the test with $\alpha_{new} = \alpha - \Delta$, where $0 < \Delta < \alpha$. In our case Δ is fixed with value 10^{-2} . In case the signal is white, stop. Notice that the bisection method cannot be used.

Running this test gives an approximate value of $c \approx 0.35 \text{ V}$. The simulated current, using the parameters identified for the motor, is shown in figure 3.2. Moreover, using the cost function mentioned at the beginning of this part, we obtain a fit value of 0.89 on the validation data (done using a different sinusoid).

3.2 Motor mechanical static friction



(a) Current vs Voltage plot



(b) Current vs Position plot

Figure 3.1: On the left: plot of the input voltage and output current. The deadzone effect on the current sets the current to 0 for small v . On the right we can see the effect on the position of the cart.

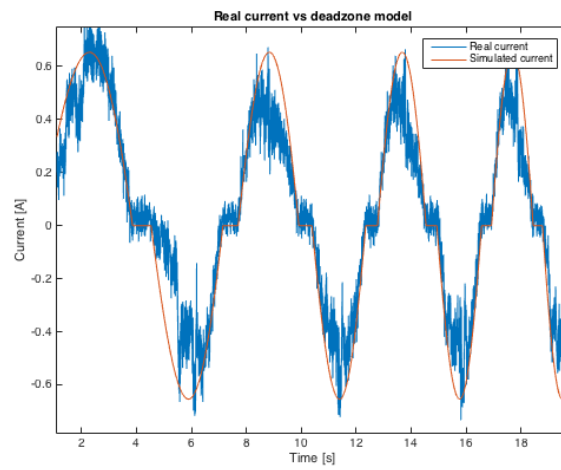


Figure 3.2: Identified model vs real current.

Chapter 4

State filtering

Part III

System control

Chapter 1

Control of 1 Degree of Freedom

1.1 PID and Classical Control

1.2 RHP-Zeros Control

During the development of the project it was apparent that using an integrator was necessary to eliminate steady state-error and reduce the effect of non-linearities due to the high-gain linearization effect induced by the integrator. Though, this led to some drawbacks, such as low cut-off frequency. This was induced by the fact that we have 2 complex poles near the imaginary axis, which are the cart natural frequencies. One of the best way to design a controller was to introduce two complex zero in order to cancel the effect of those complex poles. Another way was to use positive zeros in our controller.

It is well known from the root locus technique that zeros *attract* poles for increasing gain. Then it was observed, that, if we place positive zeros sufficiently near to the real axis, and not too far from the complex poles aforementioned, those poles with a sufficient gain would fall in a zone where the output signal response of the system would have low overshoot.

Now it's briefly described what are the drawbacks of RHP-zeros in the loop. From a frequency analysis we can get an insight of what happens: RHP-zeros add -180 degree to phase, therefore it's best to have those zeros at high frequency (thus the modulus of the zeros) to have their effect quickly dissipate without any effect. To analyze in time we need to take the partial fraction expansion. Let $G(s)$ be our system considered and $C(s)$ our controller. Then:

$$C(s) = \hat{k} \frac{(s-a)(s-\bar{a})}{s(s+p)}, a \in \mathbb{C}, p \in \mathbb{R}$$

where \bar{a} is the complex conjugate of a , and $\hat{k} = \frac{kp}{|a|^2}$, with $\mathbb{R}(a) > 0$. The closed loop transfer function is:

$$T(s) = \frac{CG(s)}{1+CG(s)} = \frac{\hat{k}(s-a)(s-\bar{a})\gamma}{s(s+p)(Ls+R)(Ms^2+Cs+K) + \hat{k}(s-a)(s-\bar{a})\gamma}$$

With output signal $y(t) = \mathcal{L}[T(s)R(s)]^{-1}$. For a certain k it's possible to stabilize the system, that can be seen using root locus technique. Notice that the motor since has a pole in $s \approx 600 \text{ rad s}^{-1}$ its term sL can be ignored. In closed loop, it is possible to demonstrate that we have 2 complex conjugate poles in the left half plane, and two negative poles on the real axis that if the gain increases more will become complex conjugate poles. Thus we have 4 poles, and the transfer function can be rewritten as:

$$T(s) = \frac{\hat{k}(s-a)(s-\bar{a})\gamma}{(s+p_1)(s+p_2)(s^2+2\alpha s+\beta)}$$

Where $p_2 > p_1 > 0$. The partial fraction expansion becomes:

$$T(s) = \frac{A}{s+p_1} + \frac{B}{s+p_2} + \frac{Cs+D}{s^2+\alpha s+\beta}$$

and in time it's:

$$y(t) = Ae^{-p_1 t} + Be^{-p_2 t} + Ce^{-\alpha t} \left(\cos(\theta t) + \frac{\frac{D}{C} - \alpha}{\theta} \sin(\theta t) \right)$$

Where $\theta^2 = \beta - \alpha^2$. Making use of the fact that for example $A = \lim_{s \rightarrow -p_1} (s + p_1)T(s)$ we obtain:

$$A = \frac{\hat{k}(-p_1 - a)(-p_1 - \bar{a})\gamma}{(-p_1 + p_2)(p_1^2 - 2\alpha p_1 + \beta)}$$

$$B = \frac{\hat{k}(-p_2 - a)(-p_2 - \bar{a})\gamma}{(-p_2 + p_1)(p_2^2 - 2\alpha p_2 + \beta)}$$

And

$$\lim_{t \rightarrow 0^+} \dot{y}(t) = \lim_{s \rightarrow \infty} sT(s) = A + B + C = 0 \Rightarrow C = -A - B$$

$$T(0) = \frac{\hat{k}a^2\gamma}{p_1 p_2 \beta} = \frac{A}{p_1} + \frac{B}{p_2} + \frac{D}{\beta}$$

It can be proven that $\text{sign } C = -\text{sign } \mathbb{R}(a)$, whilst A, B, D maintain their sign. In fact C is:

$$C = \frac{-\hat{k}\gamma}{p_2 - p_1} \left(\frac{(-p_1 - a)(-p_1 - \bar{a})}{p_1^2 - 2\alpha p_1 + \beta} - \frac{(-p_2 - a)(-p_2 - \bar{a})}{p_2^2 - 2\alpha p_2 + \beta} \right)$$

Notice that the sign of C , with the hypothesis $p_2 > p_1$, depends only on the numerator of the fractions inside the brackets (not the denominators, which are always positive):

$$C = \frac{-\hat{k}\gamma}{p_2 - p_1} \left(\frac{p_1^2 - 2p_1\mathbb{R}(a) + a^2}{p_1^2 - 2\alpha p_1 + \beta} - \frac{p_2^2 - 2p_2\mathbb{R}(a) + a^2}{p_2^2 - 2\alpha p_2 + \beta} \right)$$

For $\mathbb{R}(a) < 0 \Rightarrow C > 0$ and viceversa. This effects leads to $\dot{y}(t) < 0$ for some t , causing the *undershoot* effect.

More in general, by looking at the expression of $T(s)$, it's possible to notice that the effect of $\mathbb{R}(a)$ is visible starting from the $r + 1$ time derivative of $y(t)$, where r is the relative degree, thus $\text{sign } y^{r+1}(0) = \text{sign } \hat{k}\gamma\mathbb{R}(a)$. But derivative up to the r -th order are positive, thus for this reason the undershoot effect is delayed and does not appear right at the beginning.

Finally an even number of positive zeros display the undershoot effect after a small time. On the other hand it can be proven [1] that an odd number of positive zeros show the undershoot effect right at the start. Obviously the effect of those zeros can be reduced by moving them far away from the origin (i.e. in high frequency), where the gain of the system is very low, but, then, the root locus would change.

1.3 H_∞ control

1.4 LQG Control

1.5 Adaptive control

Chapter 2

Control of 2 Degree of Freedom

Chapter 3

Control of 3 Degree of Freedom

Conclusions

Appendix

Bibliography

- [1] Dennis S. Bernstein Jesse B. Hoagg. “On the Zeros, Initial Undershoot, and Relative Degree of Lumped-Mass Structures”. In: *Proceedings of the American Control Conference* (2006).